

Rare-Allele Detection Using Compressed Se(que)nsing

Noam Shental¹ Amnon Amir² Or Zuk³

February 8, 2022

Abstract

Detection of rare variants by resequencing is important for the identification of individuals carrying disease variants. Rapid sequencing by new technologies enables low-cost resequencing of target regions, although it is still prohibitive to test more than a few individuals. In order to improve cost trade-offs, it has recently been suggested to apply pooling designs which enable the detection of carriers of rare alleles in groups of individuals. However, this was shown to hold only for a relatively low number of individuals in a pool, and requires the design of pooling schemes for particular cases.

We propose a novel pooling design, based on a *compressed sensing* approach, which is both general, simple and efficient. We model the experimental procedure and show via computer simulations that it enables the recovery of rare allele carriers out of larger groups than were possible before, especially in situations where high coverage is obtained for each individual.

Our approach can also be combined with barcoding techniques to enhance performance and provide a feasible solution based on current resequencing costs. For example, when targeting a small enough genomic region (~ 100 base-pairs) and using only ~ 10 sequencing lanes and ~ 10 distinct barcodes, one can recover the identity of 4 rare allele carriers out of a population of over 4000 individuals.

1 Introduction

Genome-Wide Association Studies (GWAS) [29] have been successfully used in recent years to detect associations between genotype and phenotype, and numerous new alleles have been found to be linked to various human traits [7, 33, 46]. However, genotyping technologies are limited only to those variants that are predetermined and prioritized for typing, which results in a bias towards typing of *common* alleles.

¹Department of Computer Science, The Open University of Israel, Raanana, 43107, Israel
shental@openu.ac.il

²Department of Physics of Complex Systems, Weizmann Institute of Science, Rehovot, 76100, Israel
amnon.amir@weizmann.ac.il

³Broad Institute of MIT and Harvard, Cambridge, 02142, MA, USA
orzuk@broadinstitute.org

Although many common alleles were lately found to have statistically significant associations with different human traits, they were thus far shown to explain only a small fraction of most traits' heritability content. This, together with other theoretical and empirical arguments, raise the possibility that in fact *rare* alleles may play a significant role in the susceptibility of human individuals to many common diseases [5, 13, 34, 40]. Discovering and genotyping of rare alleles may therefore be of great bio-medical interest, however such studies require genotyping of large human populations - a task considered infeasible until recently.

This state of affairs may change dramatically as we are currently witnessing a rapid revolution in genome sequencing due to emerging new technologies. Sequencing throughput at a given cost is growing at an exponential rate, in similar to Moore's law for computer hardware [38]. At present next-generation sequencing technologies [26, 28, 39] utilize massively parallel reading of short genomic fragments to achieve several orders of magnitude higher throughput at the same cost as previous Sanger sequencing machines [38]. The availability of cheap, high-throughput rapid sequencing methods leads to a change in the way researchers approach various biological problems, as it enables addressing questions which were infeasible to be studied before.

Next-generation sequencing opens the possibility to obtain the genomic sequences of multiple individuals along specific regions of interest. This approach, often called resequencing, is likely to provide an extensive amount of novel information on human genetic variation. In particular, the ability to resequence a large number of individuals will enable the study of *rare* alleles in human populations. Resequencing of large populations can thus fill a gap in our knowledge by allowing us to discover and type these rare variants, often with frequencies well below 1%, at given predefined regions. Of particular interest are regions around loci that have previously been established for involvement in disease, as they can be resequenced across a large population to seek novel variations.

Another important application of interest is resequencing a set of specific *known* Single-Nucleotide-Polymorphisms (SNPs) with low minor allele frequency which are known or suspected to be important for a certain trait. In this case we are interested in identifying individuals carrying these alleles out of a very large group of individuals. For example, this may assist in scanning of large populations for individuals carrying certain risk alleles for a potentially lethal disease. For the sake of clarity in this paper we focus on this application, although discovery and typing of unknown rare variants can also be applied following the same lines.

Current next-generation sequencing technologies provide throughput on the order of millions of reads in a single 'run' or 'lane' [38], where a sequence read is typically a short consecutive DNA fragment of a few dozens to a few hundreds nucleotides. In addition, novel experimental procedures enable targeted selection of pre-defined genomic regions prior to sequencing [1, 25, 42]. These methods, also called 'hybrid capture' or 'hybrid selection', enrich significantly the DNA or RNA within the regions of interest and minimize the number of reads 'wasted' on fragments residing outside these regions. Together, these high-throughput technologies have made the identification of carriers over a pre-defined region a feasible, yet still an expensive task.

A naive but costly option is to utilize one lane per individual. However, when considering a population of hundreds or thousands of individuals, such an approach is prohibitively expensive. Moreover, since resequencing is typically performed on targeted regions rather than the whole genome, throughput requirements to sequence an individual are much lower than the capacity of a single lane, thus the naive approach is also highly inefficient.

In such cases, “pooled” sequence runs may offer a more feasible approach. In “pooled DNA” experiments, DNA from several individuals is mixed and sequenced together on a single sequencing lane. Pooled genotyping has been used to quantify previously identified variations and study allele frequency distributions in populations [43, 45, 47]. Given a measurement for each allele, it is possible to estimate the average frequency of the allele in those individuals participating in the pool. However, traditional pooled sequencing was used only to infer the *frequency* of rare alleles in a population, and did not give means to recover the *identity* of rare allele carriers. In this work we focus on the latter task, of *identifying* rare allele carriers by sequencing pooled DNA.

The field of *group testing* [18] aims to tackle this problem of identifying individuals carrying a certain trait out of a group, by designing an efficient set of test, i.e., pools. This field which dates back to the mid 20’t century has applications in biology [18], streaming algorithms [41] and communications (See [24] for a comprehensive survey.) Recently, several works have tried to use resequencing-based group testing methods in order to identify rare allele carriers.

Prabhu and Pe’er [44] offered to use overlapping pools, elegantly designed based on Error-Correcting-Codes, to enable the recovery of a single rare-allele carrier from multiple pools. Individuals are represented in multiple pools, where the composition of different pools is constructed in a way which provides a unique pooling ‘signature’ for each individual. This carefully designed scheme enables the recovery of a rare allele carrier by observing the presence of reads containing the rare allele in these ‘signature’ pools. Their design offers a significant saving in resources, as it enables the recovery of a single carrier out of N individuals, by using only $O(\log N)$ pools. It is, however, limited to the case of a single rare allele carrier within the group, and the problem of detecting multiple (albeit few) carriers remained unsolved.

In another approach by Erlich et al. [20] a clever barcoding scheme combined with pooling was used, in order to enable the identification of each sample’s genotypes. When using barcoding, each sample is “marked” by a unique short sequence identifier, i.e., barcode, thus upon sequencing one can identify the origin of each read according to its barcode, even when multiple samples are mixed in a single lane. Ideally, one could assign a different barcode to each individual sample, and then mix many samples in each lane while keeping the identity of each read based on its barcode. However, barcoding is a costly and laborious procedure, and one wishes to minimize the number of barcodes used. It was therefore suggested in [20] to barcode different pools of samples (rather than individual samples), thus allowing the barcode to identify the pool from which a certain read was obtained, but not the identity of the specific sample. Efficient algorithms based on the Chinese-Remainder-Theorem enable the accurate recovery of rare allele carriers,

where both the total number of pools and the number of individual samples participating in each pool were kept low - the identification of N individual genotypes was obtained by using $O(\sqrt{N})$ different pools with $O(\sqrt{N})$ individuals per pool.

In this work we present a different approach to recovering the identity of individuals carrying rare variants, based on Compressed Sensing (**CS**). **CS** and group testing are intimately connected [23], yet this approach was not studied in the context of rare allele identification. Our work extends the idea of recovering the identity of rare-allele carriers using overlapping pools beyond the single carrier case analyzed in [44], and deals with heterozygous or homozygous rare alleles. The **CS** pooling approach enables testing of a larger cohort of individuals, thus identifying carriers of rarer SNPs. The **CS** paradigm also adapts naturally and efficiently to the addition of barcodes. We treat barcodes as splitting a given lane into many different lanes of approximately equal sizes in terms of number of reads - thus barcoding effectively boosts our number of lanes.

Compressed Sensing [8, 15] is a new emerging and very active field of research, with foundations in statistics and optimization. New developments, updates and research papers in **CS** appear literally on a daily basis, in various websites (e.g. <http://dsp.rice.edu/cs>) and blogs (e.g. <http://nuit-blanche.blogspot.com/>). Applications of **CS** theory can be found in many distantly related fields such as magnetic resonance imaging [37], single pixel cameras [19], geophysics [36], astronomy [4] and multiplexed DNA microarrays [14].

In **CS** one wishes to efficiently reconstruct an unknown vector of values $\mathbf{x} = (x_1, \dots, x_N)$, assuming that \mathbf{x} is *sparse*, i.e., have at most s non-zero entries, for some $s \ll N$. It has been shown that \mathbf{x} can be reconstructed using $k \ll N$ basic operations termed “measurements”, where a measurement is simply the output y of the dot-product of the (unknown vector) \mathbf{x} with a known measurement vector \mathbf{m} , $y = \mathbf{m} \cdot \mathbf{x}$. By using the values of these k measurements and their corresponding \mathbf{m} ’s, it is then possible to reconstruct the original sparse vector \mathbf{x} .

Mapping of group testing into a **CS** setting is simple. The entries of \mathbf{x} contain the genotype of each individual at a specific genetic locus and are non-zero only for minor allele carriers, thus since we are interested in rare alleles \mathbf{x} is indeed sparse. A measurement in our setting corresponds to sequencing the DNA of a pool of several individuals taken together, hence the measurement vector represents the individuals participating in a given pool and the output of the measurement is proportional to the total number of rare alleles in the pool. Our basic unit of operation is a single ‘run’ or ‘lane’, which is used to sequence L pre-defined different loci in the genome, whether consecutive in one specific region, taken from different regions or surrounding different SNPs. We treat each of the L different loci separately and reconstruct L different vectors \mathbf{x} , thus the amount of computation increases linearly with the number of loci of interest.

Formulating the problem in terms of **CS** opens the door to utilizing this fascinating and seemingly almost magical theory for our purposes. In particular, from a theoretical perspective one can use **CS** bounds to estimate the number of samples and lanes needed for reconstruction, and the robustness of the reconstruction to noise. From a more practical point of view, we can apply numerous algorithms and techniques available for **CS** problems, and benefit from the development of faster and more accurate reconstruction

algorithms as the state of the art is constantly improving (see e.g. [2].) We believe that **CS** is a suitable approach for identifying rare allele carriers, and hope that this paper is merely a first step in this direction.

In this work we present results of extensive simulations which aim to explore the benefits and limitations of applying **CS** for the problem of identifying carriers of rare alleles in different scenarios. We provide a detailed model of the experimental procedure typical to next generation sequencing and find scenarios in which the benefit of applying **CS** is overwhelmingly large (up to over $\sim 70X$ improvement) compared to the naive one-individual-per-lane approach. We also show that our method can be used in addition to barcodes, and provide a significant improvement over applying each of these methods by itself.

The paper is organized as follows: Section 2 presents **CS** in the context of identifying carriers of rare alleles, and the specific details of our proposed pooling design, genotype reconstruction algorithm and the noise model reflecting the pooled sequencing process. Simulation results are presented in Section 3, and provide evidence for the efficiency of our approach along a wide range of parameters. Finally, Section 4 offers conclusions and outlines possible directions for future research.

2 Methods

We first provide a short overview of **CS**, followed by a description of its application to our problem of identifying rare alleles, and the corresponding mathematical formulation including a noise model reflecting the sequencing process. Finally we show how one performs reconstruction while utilizing barcoding.

2.1 The Compressed Sensing Problem

In a standard **CS** problem one wishes to reconstruct a sparse vector \mathbf{x} of length N , by taking k different measurements $y_i = \mathbf{m}_i \cdot \mathbf{x}$, $i = 1, \dots, k$. This may be represented as solving the following set of linear equations

$$M\mathbf{x} = \mathbf{y} \tag{1}$$

where M is a $k \times N$ *measurement matrix* or *sensing matrix*, whose rows are the different \mathbf{m}_i 's (as a general rule, we use upper-case letters to denote matrices: M, E, \dots , lower boldface letters to denote vectors: $\mathbf{x}, \mathbf{y}, \dots$ and lower case to denote scalars: x, y, x_i .)

Typically in **CS** problems, one wishes to reconstruct \mathbf{x} from a small number of measurements, i.e. $k \ll N$, hence the linear system (1) is under-determined, namely there are ‘too few’ equations or measurements and \mathbf{x} cannot be recovered uniquely. However, it has been shown that if \mathbf{x} is sparse, and M has certain properties, the original vector \mathbf{x} can be recovered uniquely from Eq. (1) [8, 15]. More specifically, a unique solution is found in case $k > Cs \log(N/s)$, where C is a constant, and s is the number of non-zero entries in \mathbf{x} . This somewhat surprising result stems from the fact that the desired solution \mathbf{x} is sparse, thus contains less ‘information’ than a

general solution. Therefore, one can ‘compress’ the amount of measurements or “sensing” operations required for the reconstruction of \mathbf{x} .

A sensing matrix which allows for a correct reconstruction of \mathbf{x} posses a property known as “Uniform Uncertainty Principle” (UUP) or Restricted Isometry Property (RIP) [9, 11]. Briefly, UUP states that any subset of the columns of M of size $2s$ form a matrix which is almost orthogonal (although since $k < N$ the columns cannot be perfectly orthogonal), which, in practice, makes the matrix M “invertible” for sparse vectors \mathbf{x} . The construction of a “good” sensing matrix is an easy task when one is able to use randomness. As an example of a UUP matrix consider a Bernoulli matrix, namely a matrix whose entries are independent random variables set to be 1 or -1 with probability 0.5^1 . It is known that almost any instance of such a random matrix will satisfy UUP with an overwhelming probability [12, 16] (the same is true when each entry in the matrix is a standard Gaussian random variable.)

Once M and \mathbf{y} are given, **CS** aims to find the sparsest possible \mathbf{x} which obeys Eq. (1). This can be written as the following optimization problem:

$$\mathbf{x}^* = \underset{\mathbf{x}}{\operatorname{argmin}} \|\mathbf{x}\|_0 \quad \text{s.t. } M\mathbf{x} = \mathbf{y} \quad (2)$$

where the ℓ_0 norm $\|\mathbf{x}\|_0 \equiv \sum_i 1_{\{x_i \neq 0\}}$ simply counts the number of non-zero elements in \mathbf{x} .

Problem (2) involves a non-convex ℓ_0 term and can be shown to be computationally intractable in general [10]. However, another impressive breakthrough of **CS** theory is that one can relax this constraint to the closest convex ℓ_p norm, namely the ℓ_1 norm, and still get a solution which, under certain conditions, is identical to the solution of problem (2). Hence the problem is reformulated as the following ℓ_1 minimization problem, which can be efficiently solved by convex optimization techniques:

$$\mathbf{x}^* = \underset{\mathbf{x}}{\operatorname{argmin}} \|\mathbf{x}\|_1 \quad \text{s.t. } M\mathbf{x} = \mathbf{y} \quad (3)$$

In most realistic **CS** problems measurements are corrupted by noise, hence Eq. (1) is replaced by $M\mathbf{x} + \boldsymbol{\eta} = \mathbf{y}$, where $\boldsymbol{\eta} = (\eta_1, \dots, \eta_k)$ are the unknown errors in each of the k measurements, and the total measurement noise, given by the ℓ_2 norm of $\boldsymbol{\eta}$ is assumed to be small. Therefore, the optimization problem is reformulated as follows:

$$\mathbf{x}^* = \underset{\mathbf{x}}{\operatorname{argmin}} \|\mathbf{x}\|_1 \quad \text{s.t. } \|M\mathbf{x} - \mathbf{y}\|_2 \leq \epsilon \quad (4)$$

where $\epsilon > 0$ is set to be the maximal level of noise we are able to tolerate, while still obtaining a sparse solution. It is known that **CS** reconstruction is robust to noise, thus adding the noise term ϵ does not cause a breakdown of the **CS** machinery, but merely leads to a possible increase in the number of measurements k [9].

Many efficient algorithms are available for problem (4) and enable a practical solution even for large matrices, with up to tens of thousands of rows. We have chosen to work with the commonly used GPSR algorithm [21].

¹It is common to require orthonormality of the columns therefore the entries should also be divided by \sqrt{k} .

2.2 Rare-Allele Identification in a CS Framework

We wish to reconstruct the genotypes of N individuals at a specific locus. The genotypes are represented by a vector \mathbf{x} of length N , where x_i represents the genotype of the i th individual. We denote the reference allele by A , and the alternative allele by B . The possible entries of x_i are 0, 1 and 2, representing a homozygous reference allele (AA), a heterozygous allele (AB) and a homozygous alternative allele (BB), respectively. Hence, x_i counts the number of (alternative) B alleles of the i th individual, and since we are interested in rare minor alleles, most entries x_i are zero. In classic **CS** the unknown variables are typically real numbers. The restriction on \mathbf{x} in this case is expected to reduce the number of measurements needed for reconstruction and may also enable using faster reconstruction algorithms, as it is known that even a weaker restriction, namely that all entries are positive, already simplifies the reconstruction problem [17].

The sensing matrix M is built of k different measurements represented by the rows of M . The entry m_{ij} is set to 1 if the j th individual participates in i th measurement, and zero otherwise. Each measurement includes a random subset of individuals, where the probability to include a certain individual is 0.5. Hence, M is equivalent to the Bernoulli matrix mentioned in Section 2.1, which is known to be a “good” sensing matrix² (another type of a sensing matrix, in which only $\sim\sqrt{N}$ elements in each measurement are non-zero is considered in Section 3).

In practice, measurements are performed by taking equal amounts of DNA from the individuals chosen to participate in the specific pool, thus their contribution to the mixture is approximately equal. Then, the mixture is amplified using PCR, which ensures that the amplification bias generated by the PCR process affects all individuals equally [30]. Finally, DNA of each pool is sequenced in a separate lane, and reads are mapped back to the reference genome (this may be performed using standard alignment algorithms such as MAQ [35].) For each locus of interest we record the number of reads containing the rare allele together with the *total* number of reads covering this locus in each pool, denoted by r . These numbers provide the measurement vector \mathbf{y} representing the k frequencies obtained for this locus in the k different pools. The measurement process introduces various types of noise which we model in the next section.

For each locus, our goal is to reconstruct the vector \mathbf{x} , given the sensing matrix M and the measurement vector \mathbf{y} , while realizing that some measurement error ϵ is present (see Eq. (4).) Our experimental design is illustrated in Fig. 1, and the following section describes its mathematical formulation.

2.3 Mathematical Formulation of Our Model

The model presented here, including the range of parameters chosen, aims at reflecting the sequencing process by the Illumina technology [26], but may also be applied to other next generation technologies as well. It is similar, but not identical, to the model presented in [44]. For clarity of presentation, we first describe our model while ignoring the different experimental noise factors, and these are added once the model is established.

²This is easily seen by using the simple linear transformation $x \rightarrow (2x - 1)/\sqrt{k}$.

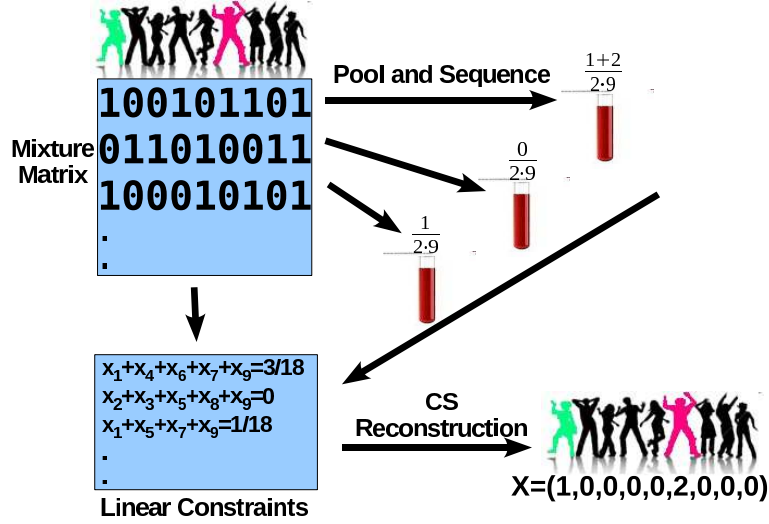


Figure 1: Schematics of the CS based pooling method. Consider the case of 9 people, out of which one is a heterozygotic carrier of the rare SNP (marked green), and another one who is a homozygous alternative allele carrier (marked red.) Each sample is randomly assigned to a pool with probability 0.5, as described by the sensing matrix. For example, individuals 1, 4, 6, 7 and 9 are assigned to the first pool. The DNA of the individuals participating in each pool is mixed, and the fraction of rare alleles in each pool is measured. For example, the first pool contains the two carriers, hence the frequency of the B' s is $1+2$ out of the 2×9 alleles. The sensing matrix and the resulting frequencies are incorporated into an underdetermined set of linear constraints, from which the original rare SNP carriers are reconstructed.

Let \mathbf{x} be the unknown sparse genotypes vector, as described in Section 2.2. The fraction of individuals with the rare allele is denoted f , thus the vector \mathbf{x} has $s = fN$ non-zero elements³. M is a $k \times N$ Bernoulli sensing matrix, and denote by \hat{M} the normalized version of M whose entries represent the fraction of each individual's DNA in each pool:

$$\hat{m}_{ij} \equiv \frac{m_{ij}}{\sum_{j=1}^N m_{ij}} \quad (5)$$

Assume that the mixing of DNA is perfect and unbiased, and that each DNA segment from each individual in a pool is equally likely to be read by the sequencing machinery. Suppose that a read from the i 'th pool is drawn from a DNA segment covering our desired locus. It is then expected that this read will contain the B allele with probability $q_i \equiv \frac{1}{2} \hat{\mathbf{m}}_i \cdot \mathbf{x}$, where $\hat{\mathbf{m}}_i$ is the i 'th row of \hat{M} (the $\frac{1}{2}$ pre-factor is due to the fact that both alleles are sequenced for each individual.) The vector of frequencies of the B allele, for each of the k pools is therefore:

$$\mathbf{q} = \frac{1}{2} \hat{M} \mathbf{x} \quad (6)$$

Had we been able to obtain a full and error-free coverage of the DNA present in the pool, our measurements would have provided us with the exact value of \mathbf{q} . In practice a specific position is covered by a limited number of reads, which we denote by r , and the

³Here and throughout the paper we define the fraction of *individuals* (rather than alleles) as the 'rare-allele-frequency' - thus the fraction of alternative *alleles*, assuming Hardy-Weinberg (HW) equilibrium, is in fact $1 - \sqrt{1 - f}$.

number of reads from the rare alleles \mathbf{z} out of the total number of reads r is binomially distributed $z_i \sim \text{Binomial}(r, q_i)$. Generally, one can only control the expected number of reads covering a specific locus, as also r is considered a random variable. The main cause for variation in r is the different amplification biases for different regions, which are effected by properties such as a region's GC-content. The distribution of r over different loci depends on the experimental conditions, and was shown to follow a Gamma distribution in certain cases [44]. We adopt this assumption, draw r for each locus from a Gamma distribution $r \sim \Gamma(\frac{R}{L}, 1)$, and apply it to all k pools.

This binomial sampling process provides measurements which are close, yet not identical to the expected frequency of the rare allele $r q_i$, and these fluctuations are regarded as *sampling noise*. Therefore the **CS** problem formulation is given by (compare to Eq. (4)):

$$\mathbf{x}^* = \underset{\mathbf{x} \in \{0,1,2\}^N}{\operatorname{argmin}} \|\mathbf{x}\|_1 \quad \text{s.t.} \quad \|\frac{1}{2}\hat{M}\mathbf{x} - \frac{1}{r}\mathbf{z}\|_2 < \epsilon \quad (7)$$

Adding noise factors. The model described so far assumes that no noise or bias exist in our setting, besides sampling noise which is related to the limited number of reads. In a more realistic scenario, we do expect additional noise factors to be present due to imperfection in experimental procedures. We have modeled these factors by adding two more types of noise: sequencing read errors and errors in DNA preparation.

Read error models the noise factors introduced throughout the process of sequencing by next generation techniques such as Illumina, and reflect the fact that reads obtained from the sequencing machine may not match the DNA molecule sampled. This can be due to errors in certain bases present in the read itself, mis-alignment of a read to a wrong place in the genome, errors introduced by the PCR amplification process (which are known to introduce base substitutions in the replicated DNA [22]), or any other unknown factors. All of these can be modeled using a single parameter e_r , which represents the probability that the base read is different from the base of the measured sample's DNA at a given locus. The resulting base can be any of the other three different nucleotides, however we conservatively assume that the errors will *always* produce the alternative allele B (if, for example the reference allele is 'G' and the alternative allele is 'T', we assume that all erroneous reads produce 'T'. In practice, some reads will produce 'A' and 'C', and these can be immediately discarded thus reducing the effective error rate.) The probability of observing B at a certain read is therefore obtained by a convolution of the frequency of B alleles and the read error:

$$\mathbf{q} = (1 - e_r)\frac{1}{2}\hat{M}\mathbf{x} + e_r(1 - \frac{1}{2}\hat{M}\mathbf{x}) \quad (8)$$

The value of e_r may vary as a function of the sequencing technology, library preparation procedures, quality controls and alignment algorithms used. Typical values of e_r , which represent realistic values for Illumina sequencing [31], are in the range $e_r \sim 0.5\% - 1\%$. We assume that e_r is known to the researcher, and that it is similar across different lanes. In this case, one can correct for the convolution in Eq. (8) and obtain the following problem:

$$\mathbf{x}^* = \underset{\mathbf{x} \in \{0,1,2\}^N}{\operatorname{argmin}} \|\mathbf{x}\|_1 \quad \text{s.t.} \quad \|\frac{1}{2}\hat{M}\mathbf{x} - (\frac{1}{r}\mathbf{z} - e_r)/(1 - 2e_r)\|_2 < \epsilon \quad (9)$$

Hence the measurement vector in our problem equals $\mathbf{y} = (\frac{1}{r}\mathbf{z} - e_r)/(1 - 2e_r)$ and the sensing matrix is $\frac{1}{2}\hat{M}$. If e_r is unknown, one may still estimate it, for example by running one lane with a single region on a single individual with known genotypes. Alternatively, we show in Appendix A how to incorporate the estimation of the read error term e_r within our **CS** framework from the overlapping pooled sequence data. The noise factors described thus far (including sampling noise and read errors) resembles the one proposed previously in [44].

Finally we add to our model one more source of noise, namely DNA preparation errors (DP errors.) This error term reflects the fact that in an experimental setting it is hard to obtain exactly equal amounts of DNA from each individual. The differences in the actual amounts taken result in noise in the measurement matrix M . While M is our original zero-one Bernoulli matrix, the actual measurement matrix M' is obtained by adding DP errors to each non-zero entry. Hence, the true mixture matrix is $M' \equiv M + D$, where the DP matrix D adds a centered Gaussian random variable to each non-zero entry of M :

$$d_{ij} \sim \begin{cases} N(0, \sigma^2) & \text{if } m_{ij} = 1 \\ \equiv 0 & \text{otherwise.} \end{cases} \quad (10)$$

We consider values of σ in the range of 0–0.05 reflecting up to $\sim 5\%$ average noise on the DNA quantities of each sample. The matrix M' is unknown and we only have access to M , hence the form of Eq. (9) in this case is unchanged. M' takes effect indirectly by modifying \mathbf{q} , which effects \mathbf{z} the actual number of reads from the rare allele. As opposed to a classic **CS** problem in which the sensing matrix is usually assumed to be known exactly, DP effectively introduces noise into the matrix itself. We study this effect of DP errors in Section 3, and show that a standard **CS** approach is robust to such noise.

Targeted region length and coverage considerations. The expected number of reads from a certain locus is determined by the total number of reads in a lane R and the number of loci covered in a single lane L , and is given by $E[r] = \frac{R}{L}$ (the actual number of reads from each locus r follows a Gamma distribution with mean $\frac{R}{L}$.)

L is determined by the size of the regions and the number of SNPs of interest in a given study, and by the ability of targeted selection techniques [1, 25, 42] to enrich for a given small set of regions. We consider L as a parameter and study its effect on the results. When we treat different isolated SNPs, L indeed represents the number of SNPs we cover, as each read covers one SNP. When interested in contiguous genomic regions, however, L should be interpreted as the length of the target region in *reads*, rather than nucleotides, since each read covers many consecutive nucleotides. Therefore one should multiply L by the read length. For example, if our reads are of length 50 nucleotides, and L is taken to be 100, we in fact cover a genomic region of length 5kb.

R is defined as the number of reads which were successfully aligned to our regions of interest. It is mostly determined by the sequencing technology, and is in the order of millions for modern sequencing machines. R is also greatly influenced by the targeted selection techniques used, and since these are not perfect, a certain fraction of reads might not originate from the desired regions and is thus ‘wasted’. The total number of reads varies according to experimental protocols, read length and alignment algorithms

but is typically on the order of a few millions. Throughout this paper we have fixed R to be $R = 4000000$, representing a rather conservative estimate of a modern Illumina genome analyzer's run (e.g. compare to [38]), and also assuming that targeted selection efficiency is very high (it is reported to be $\sim 90\%$ in [25].) Other values of R may be easily dealt with using our simulation framework, thus adapting to a particular researcher's needs.

Another important and related parameter is the *average coverage per individual per SNP*, denoted c , which is given by:

$$c = \frac{R/L}{N/2} \left(\equiv \frac{E[r]}{N/2} \right) \quad (11)$$

Our model does not directly use c and it is provided merely as a rough estimate for the coverage in Section 3, as it can be easily interpreted and compared to coverage values quoted for single sample sequencing experiments. When the total number of reads in a pool r is given, the actual coverage obtained for each person in a pool has a distribution which is approximately $\text{Binomial}(r, 1/N_{\text{pooled}})$, where $N_{\text{pooled}} \sim \frac{N}{2}$ is the number of individuals in the pool. Therefore the average coverage per individual in a given pool is indeed approximately c .

2.4 Example

In order to visualize the effect of the three noise factors, i.e., sampling noise, read errors and DP errors, Fig. 2 presents the measured values \mathbf{y} in a specific scenario. We simulate an instance of $N = 3000$ individuals and rare allele frequency $f = 0.1\%$, tested over $k = 100$ lanes. Hence we have three heterozygotic carriers to be identified, and, in the absence of noise, the measurement in each lane should display four levels, which correspond to whether 0, 1, 2 or 3 of the carriers are actually present in the specific pool.

In order to display the effect of sampling noise, we consider three values for the average coverage c , i.e., number of reads per individual per SNP: 27, 267 and an infinite number of reads, which corresponds to zero sampling noise. Each of these three values appears on a separate row in Fig. 2. The panels on the left hand side of Fig. 2 correspond to read error $e_r = 1\%$, while on the right hand side there is no read error at all. The data in all panels contain DP errors with $\sigma = 0.05$. Each panel also displays the actual number of reconstruction errors in each case, namely the Hamming distance between the correct vector \mathbf{x} and reconstructed vector \mathbf{x}^* obtained by solving Eq. (9).

The effect of sampling noise is clearly visible in Fig. 2. An infinite amount of reads (lower row; (e),(f)), causes the measurements to be very close to their expected frequency, where slight deviations are only due to DP errors and the fact that the pool size is not exactly $N/2$. For a moderate number of reads ($c = 267$ - middle row; (c),(d)) the measurements follow the expected frequency levels when there are no read errors (right panel (d)), but this rough quantization completely vanishes for $e_r = 1\%$ (left panel (c).) However, reconstruction was accurate even in this case, because our **CS** formulation (Eq. (9)) takes these errors into account and aggregate the information from *all* lanes to

enable reconstruction. When the number of reads per person is small ($c = 27$ - upper row; (a),(b)), the four levels disappear irrespective of the read error. Reconstruction is still accurate in the absence of read errors (right panel (b)), and there are 4 errors in the reconstructed genotype vector \mathbf{x}^* when $e_r = 1\%$ (left panel (a)), which probably implies that sampling noise is too high in this case. While a coverage of 27 reads per person is overwhelmingly sufficient when sequencing a *single* individual, it leads to errors in the reconstruction when pooling many individuals together.

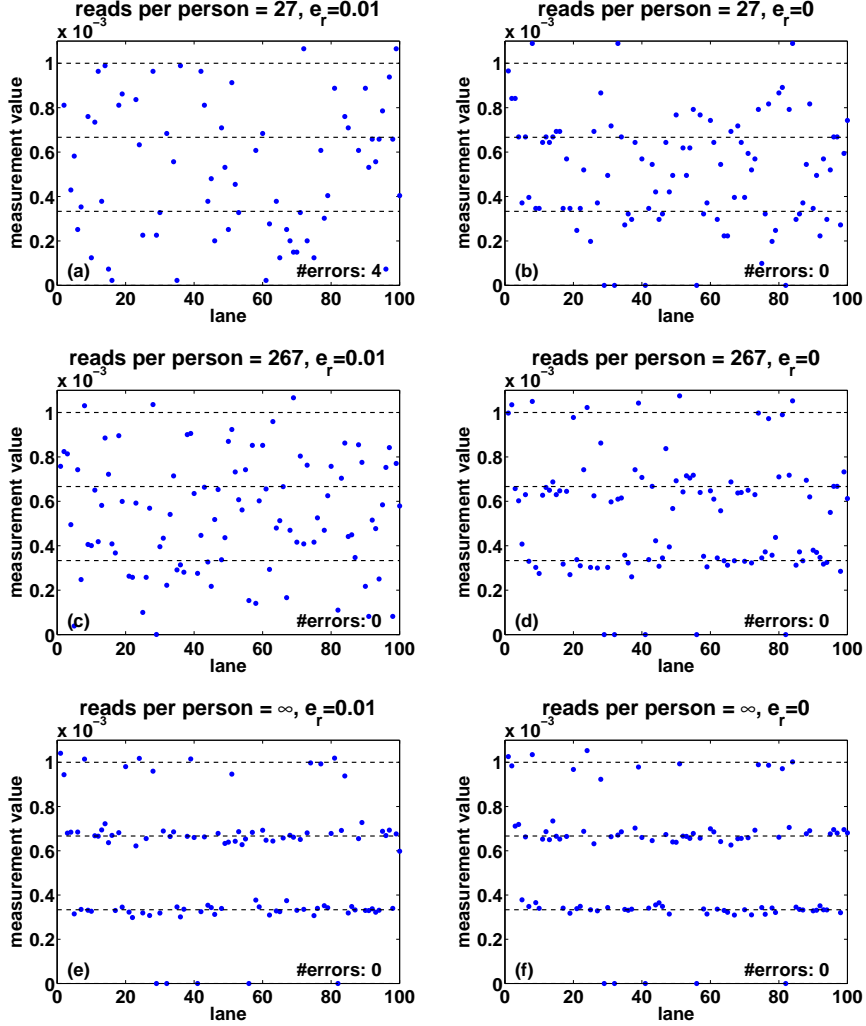


Figure 2: The values measured for 100 different pools, for a specific case of $N = 3000$ individuals and rare allele frequency $f = 0.1\%$, thus 3 individuals carry the alternative allele. Shown are the measured rare-allele frequencies in each lane, for different coverage levels, (27, 267 and ∞ reads per pool), and different values of the read error ($e_r = 0\%, 1\%$). The data in all panels contain DP errors with $\sigma = 0.05$. The dashed lines represents the possible expected frequencies corresponding to 0, 1, 2, 3 rare-allele carriers in a pool - these are the values we would have obtained in the absence of read error, DP errors, and assuming that each pool contains exactly $N/2$ individuals. The coverage r (i.e. number of reads) is the most dominant factor causing deviations of the observed values from their expectancy.

2.5 Reconstruction

We use the Gradient Projection for Sparse Reconstruction algorithm (GPSR) [21], to solve the optimization problem (9). GPSR is designed to solve a slightly different, but equivalent, formulation as in Eq. (9):

$$\mathbf{x}^* = \underset{\mathbf{x}}{\operatorname{argmin}} \quad \left\| \frac{1}{2} \hat{M} \mathbf{x} - \left(\frac{1}{r} \mathbf{z} - e_r \right) / (1 - 2e_r) \right\|_2 + \tau \|\mathbf{x}\|_1 \quad (12)$$

where the parameter τ provides the trade-off between the equations fit and the sparsity promoting factor, and is equivalent to specifying the maximal allowed error ϵ . It is often desirable in applications to let the parameter τ scale with $\|\hat{M}^T \mathbf{y}\|_\infty$ [32], where in our case $\mathbf{y} = (\frac{1}{r} \mathbf{z} - e_r) / (1 - 2e_r)$ corresponds to the measurements. We have chosen to adopt this scaling throughout this paper, and have set $\tau = 0.01 \|\hat{M}^T \mathbf{y}\|_\infty$, although experimentation with different values of τ did not alter results significantly.

GPSR outputs a sparse vector \mathbf{x}^* with a few non-zero real entries, but does not use the fact that our variables are integers from the set $\{0, 1, 2\}$. We therefore perform a post-processing step in order to obtain such a solution. Simple rounding of the continuous results in \mathbf{x}^* may obtain such a vector⁴. We chose a different post-processing scheme, which yields better performance: we rank all non-zero values obtained by GPSR, and round the largest s non-zero values, setting to zero all other $N - s$ values to get the vector \mathbf{x}^{*s} . We then compute an error term $err_s \equiv \left\| \frac{1}{2} \hat{M} \mathbf{x}^{*s} - \mathbf{y} \right\|_2$. Repeating this for different values of s we select the vector \mathbf{x}^{*s} which minimizes the error term err_s . Thus the final solution's sparsity s is always smaller or equal to the sparsity of the vector obtained by GPSR.

2.6 Utilizing Barcodes

In this section we describe how a **CS**-based method can be combined with a barcoding strategy resulting in improved performance. A barcode is obtained by attaching to the DNA in each sample a unique DNA sequence of about 5 additional nucleotides, which enables the unique identification of this sample [27]. Hence samples with different barcodes can be mixed together into a single lane, and reads obtained from them can be uniquely attributed to the different samples. In a pooled-barcode design [20], the DNA in each pool (as opposed to the DNA of a specific individual) is tagged using a unique barcode. If n_{bar} different barcodes are available, we may apply n_{bar} pools to a single lane and still identify the pool from which each read originated (although not the specific individual.)

We utilize barcodes by increasing the number of effective lanes while the number of reads per lane is decreased. The usage of k lanes and n_{bar} barcodes is simply translated into solving problem (9) with $k \times n_{bar}$ pools and R/n_{bar} total reads per lane. Barcodes can therefore be combined easily with our **CS** framework so as to improve efficiency. We did not try to estimate the relative cost of barcodes and lanes as it may vary according to

⁴by ‘rounding’ here we mean reducing to the set $\{0, 1, 2\}$. Thus any negative number is ‘rounded’ to zero and any number larger than 2 is ‘rounded’ to 2.

lab, timing and technology conditions. We therefore solve the **CS** problem for different (k, n_{bar}) combinations, thus presenting the possible trade-offs.

2.7 Simulations

We have run extensive simulations in order to evaluate the performance of our approach. Various parameter ranges were simulated, where each set of parameters was tested in 500 instances. In each simulation we have generated an input genotype vector \mathbf{x} , applied measurements according to our mathematical model, and have tried to reconstruct \mathbf{x} from these measurements. In order to evaluate the performance of our approach, one needs a measure of reconstruction accuracy, reflecting the agreement between the input vector \mathbf{x} and the reconstructed **CS** vector \mathbf{x}^* (even when executing the naive and costly approach of sequencing each individual in a separate lane, one still expects possible disagreements between the original and reconstructed vectors due to insufficient coverage and technological errors.) Each entry i for which x_i is different from x_i^* is termed a reconstruction error, and implies that the genotype for a certain individual was not reconstructed correctly, yielding either a false positive ($x_i = 0 \neq x_i^*$) or a false negative ($x_i \neq 0 = x_i^*$). For simplicity, we have chosen to show a simple and quite restrictive measure of error: we distinguish between two ‘types’ of reconstructions - completely accurate reconstructions which have *zero* errors, and reconstructions for which at least one error occurred.

A certain value of the problem’s parameters (such as number of individuals, number of lanes, read error etc.) is termed “successful” if at least 95% of its instances (i.e. 475 out of 500) had *zero* reconstruction errors, namely *all* individual genotypes were reconstructed correctly. Thus, even when testing for a few thousand individuals, we require that none of the reference allele carriers will be declared as a rare allele carrier. In particular, this requirement guarantees that the False-Discovery-Rate of discovering rare-allele carriers will not exceed 0.05.

Performance is then measured in terms of N_{max} , defined as the maximal number of individuals which allow for a “successful” reconstruction, for certain values of the problem’s parameters.

3 Results

To explore the advantages of applying **CS** for efficiently identifying carriers of rare alleles, we performed various computer simulations of the experimental procedure described in Section 2.

In each instance of the simulations we set the following parameters: The number of individuals grouped together N varied between 100 and 20000. Rare allele frequency f was chosen to be 0.1%, 1% and 2%, thus in each instance we randomly select $s = Nf$ carriers, and this determines our input vector \mathbf{x} . Since rare allele frequency is low, we mostly consider the case of a heterozygous allele (AB), hence \mathbf{x} is a binary vector, with

1's marking the carriers⁵. The case of a homozygous alternative allele (BB) is presented in Section 3.1.2, thus in this case \mathbf{x} can also contain the value 2. The number of lanes k varied between 10 and 500, and L , the number of targeted loci on the same lane was 1, 10, 100 and 500 (corresponding to targeted regions of length 100 base-pairs to 50kb, assuming each read is of length 100), which leads to different levels of coverage and sampling noise. The other noise factors are kept fixed, with read error $e_r = 1\%$ and DP errors $\sigma = 0.05$, unless specified otherwise.

In Section 3.1 we estimate the performance of **CS** given all relevant noise factors, while in Section 3.2 we evaluate the individual effect of each of the three noise factors, i.e., sampling noise, read errors and DP errors. Section 3.3 shortly presents the effect of using a different sensing matrix in which only $\sim \sqrt{N}$ individuals participate in each pool, instead of $\sim N/2$. Finally, in Section 3.4 the effect of combining barcodes and **CS** is presented.

3.1 Performance of the ‘standard’ experimental setup

Figures 3,6 present N_{max} as a function of k , for different numbers of SNPs sequenced together on the same lane. The case $f = 0.1\%$ displays a different behavior than $f = 1\%$ and $f = 2\%$ and is considered separately.

3.1.1 $f = 0.1\%$

The advantages of **CS** appear most dramatically in the case of rare alleles, e.g., for $f = 0.1\%$ in Fig. 3. Each panel in Fig. 3 presents N_{max} as a function of k , for different numbers of SNPs L . The number of rare-allele carriers tested in this case were 1, 2, ..., 20, leading to $N = 1000, 2000, \dots, 20000$. The vertical right axis displays the corresponding average coverage c , obtained via Eq. (11). The thick black line in each figure is simply the line $y = x$, demonstrating the performance of the naive approach of using a single lane per sample.

When the number of available lanes is large, we can successfully identify the carriers in groups of up to 9000 or 20000 individuals, for $k = 500$ lanes, and $L = 10$ or $L = 1$, respectively (Fig. 3(a,b).) In case the number of available lanes is small we can still identify a single carrier out of 1000 individuals with merely $k = 20$ lanes, for $L = 1$ and $L = 10$. (inset in Fig. 3(a,b).) With $k = 30, 40$ lanes, we can identify 2 or 3 carriers in a group of 2000 or 3000, for $L = 1, 10$, respectively.

As is evident from the four panels of Fig. 3, N_{max} decreases as a function of L . For example, 500 lanes are sufficient to deal with 20000 individuals for $L = 1$, but only with 1000 individuals for $L = 500$. This results from insufficient coverage which causes an increase in sampling noise. Increasing the number of lanes can overcome this under-sampling as the value of N_{max} increases almost linearly with k in most cases.

In order to quantify the advantage of applying **CS** we define an “efficiency score”, presented in Fig. 4, which is simply N_{max}/k , i.e., the number of individuals for which

⁵Assuming a given locus follows HW equilibrium, the expected frequency of homozygous rare allele carriers is $(1 - \sqrt{1-f})^2 \sim f^2/4$ which is extremely low.

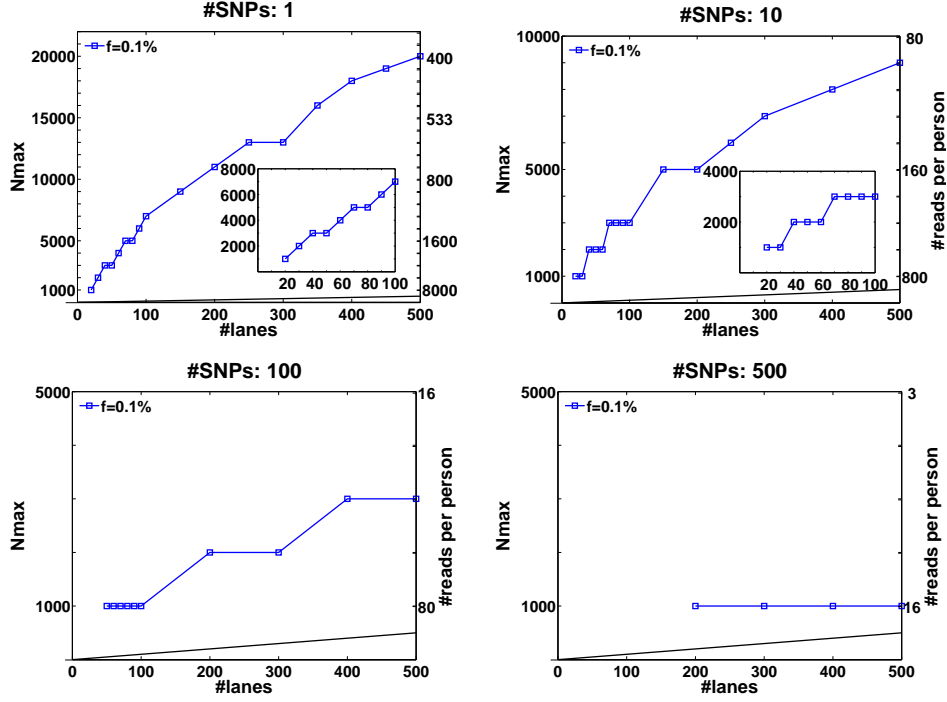


Figure 3: The maximal number of individuals N_{max} which allow for a “successful” reconstruction as a function of the number of lanes used, for different numbers of loci treated simultaneously. A “successful” reconstruction means that for a certain set of parameters at least 475 out of 500 simulations yield *zero* reconstruction errors. The black line is simply the line $y = x$, demonstrating the performance of the naive approach of using a single lane per sample. The vertical right axis displays the corresponding average coverage c for every value of N_{max} , obtained via Eq. (11). The bottom-right panels in (a) and (b) are zooming in on the region where the number of lanes is small, which is at present the most realistic scenario (in panel (c) N_{max} was constant for low numbers of lanes.) The values of N_{max} in this case were taken in units of 1000 individuals, which correspond to single carriers. Cases which appear to be missing, e.g. $k < 200$ for $L = 500$ simply mean that $N_{max} < 1000$.

reconstruction can be performed using the **CS** approach for a given number of lanes, divided by the number of individuals which can be treated using the naive one-individual-per-lane approach. Therefore, the higher the score, the more beneficial it is to apply **CS**. The black line in each plot has a value of 1 which corresponds to the naive scenario of one individual per lane. When considering up to $L = 100$ SNPs, the efficiency score is around or above 10, and in some cases is as high as 70.

The axis on the right hand side of Fig. 3 displays the average number of reads per person, i.e., average coverage c , for the relevant N_{max} . One important question is related to the optimal number of reads which allows for successful reconstruction: the smaller the coverage the more SNPs we can test on the same lane, yet we are more prone to (mostly sampling) noise. However, one can overcome the effects of low coverage by increasing the number of lanes, hence it is interesting to test the performance for each combination of coverage c and number of lanes k . In Fig. 5 we present this performance for $N = 2000$ individuals and $f = 0.1\%$. For each pair of coverage and number of lanes k we color code the percentage of instances for which there were errors in **CS** reconstruction. An

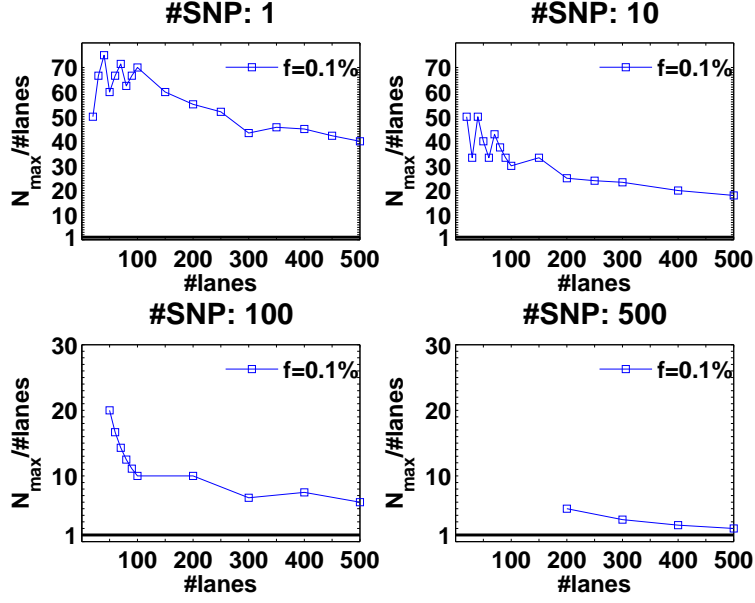


Figure 4: Efficiency score for our approach. The ratio N_{\max}/k in our approach and the number treated in the naive approach (equal to the number of lanes.) This represents the ratio of saved resources (lanes.) Efficiency is highest when a few lanes are used, and decreases gracefully as we use more and more lanes. Efficiency is highest when the targeted number of loci is small, as in this case each lane provides very high coverage.

improvement in performance may be achieved both by increasing the coverage and by increasing the number of lanes. The white line marks the 95% accuracy threshold. The transition between “successful” and “unsuccessful” reconstruction is rather sharp. For low coverage, e.g., lower than 100 reads per person, a very high number of lanes is needed in order to overcome sampling noise.

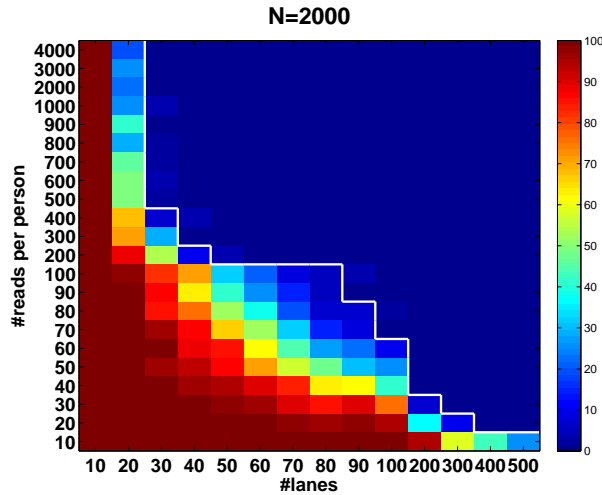


Figure 5: Performance as a function of the number of lanes k and the average coverage c . Shown is the percentage of runs in which (even a single) reconstruction error occurred. A rather sharp transition is shown, where above the white line we achieve a completely accurate reconstruction in at least 95% of the simulations. Notice the non-linearity of scale in both axes.

3.1.2 $f = 1\%$, $f = 2\%$

Figure 6 presents the results for $f = 1\%$ and $f = 2\%$. In this case the values of N tested were 100, 200, \dots , 4000 (no successful reconstruction according to our criteria was achieved for $N > 4000$.) The resulting N_{max} is lower than for the case of $f = 0.1\%$, although still much higher than in the naive approach. Results for $L = 1$ are similar to those of $L = 10$, namely increasing the coverage does not improve performance significantly in this case. The differences between results for $f = 1\%$ and $f = 2\%$ are rather small. The “efficiency score” in this case is lower (see Fig. 7), and is around 5, still offering a considerable saving compared to the naive approach.

All former simulations considered the case of identifying carriers of a heterozygous allele (AB). In order to study the possibility of also identifying homozygous alternative alleles (BB) via **CS** we simulated the following case: 1% of the individuals are BB in addition to 1% which are AB (this gives a vastly higher frequency of BB than is expected to be encountered in practice, and was taken as an extreme case to test the robustness of our reconstruction results.) The results are marked as “1% + 1%” in Figs. 6,7. Our **CS** framework deals with this scenario in exactly the same way as the other AB cases, although the results are, as expected, slightly worse than that of 2% heterozygous carriers.

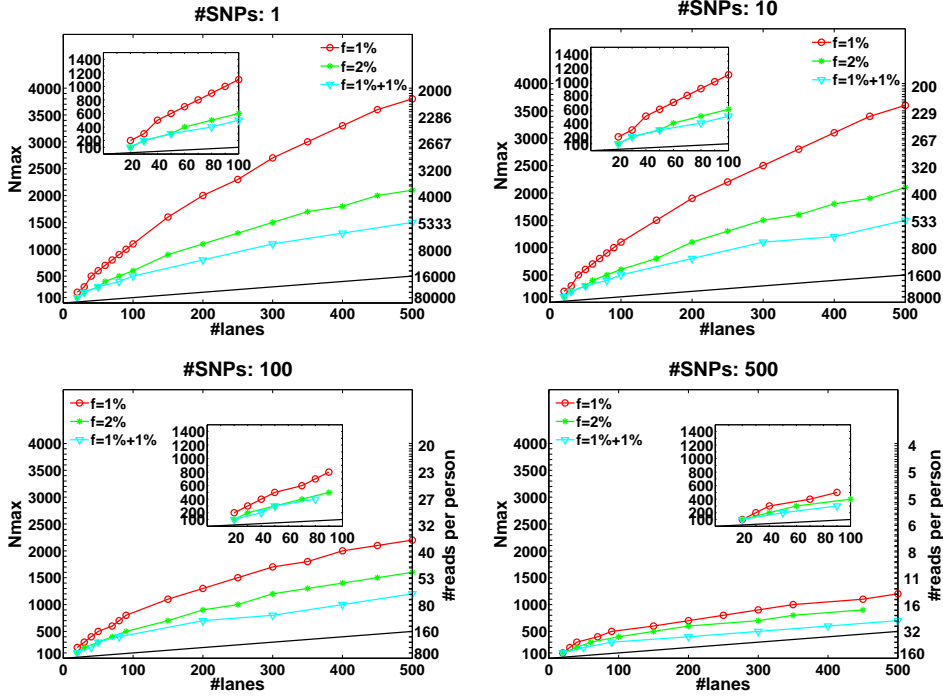


Figure 6: The maximal number of individuals N_{max} as a function of the number of lanes. Similar to Fig. 3 but with a higher frequency for the rare allele, $f = 1\%$ and $f = 2\%$. The number of individuals N_{max} achieved decreases as we increase the rare allele frequency, but we are still able to treat a much larger sample size than the naive approach. For example, one can use 40 lanes for $L = 100$ and recover 4 rare-allele carriers out of 400 ($f = 1\%$, zoomed-in view in panel(c).) The case $f = 1\% + 1\%$ corresponds to 1% AB and 1% of BB alleles.

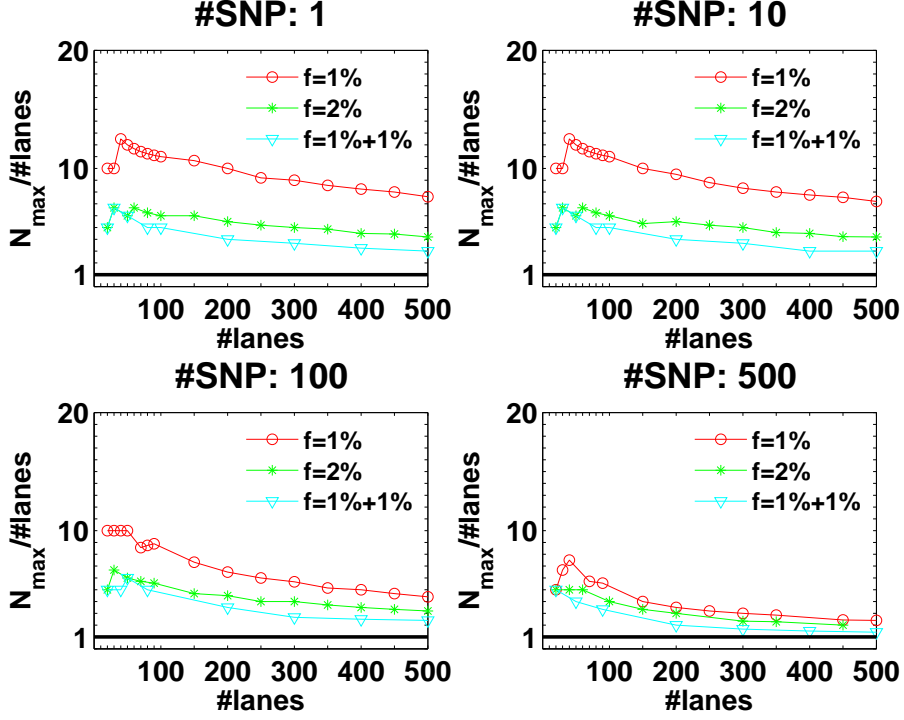


Figure 7: Efficiency score of our approach. Similar to Fig. 4 but with rare allele frequency of 1% and 2%. As expected, efficiency is decreased as rare allele frequency increases. We still reach up to 13X and 7X improvement over the naive approach for rare allele frequencies of 1% and 2% respectively.

3.2 The effect of noise

Figures 8,9 present the effects of three types of noise in the specific case of $f = 1\%$. In both figures the reference is the “standard” performance of $f = 1\%$ which appeared before in Fig. 6, and includes sampling noise, read error ($e_r = 1\%$) and DP errors ($\sigma = 0.05$). We consider the case of sampling error separately from the other two sources, as its impact is different.

3.2.1 Sampling error

Figure 8 compares the “standard” performance to the case where an infinite number of reads are available (although read error and DP errors are still present.) Differences between the cases appear only when the number of SNPs is high, thus the number of reads per person c is insufficient. In these cases N_{\max} is reduced by a factor of 2 to 4 with respect to an infinite coverage. When the number of SNPs is small, and coverage is high, we see no difference between the “standard” performance and the infinite read case.

3.2.2 Read errors and DP errors

Figure 9 compares the “standard” performance to two cases: one in which $e_r = 0$ and another in which $\sigma = 0$. In the absence of read errors N_{\max} may be twice as large as when $e_r = 1\%$. Read errors take a significant effect on performance only when L

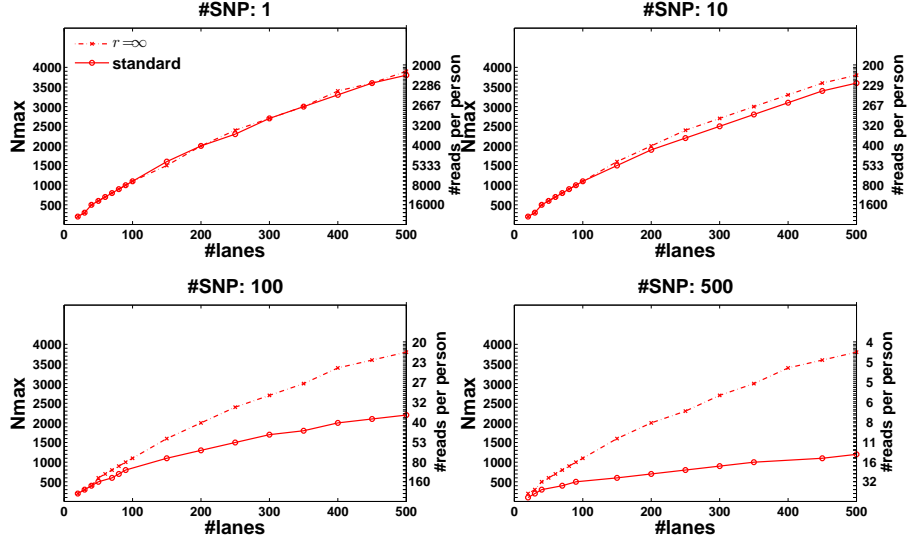


Figure 8: Effect of sampling error. The dashed line represent results obtained in the limit where the number of reads goes to infinity thus sampling error is zero. The solid line represents the realistic scenario with the current number of reads used. Sampling error is seen to be a significant factor when we treat many loci together in the same lane ($L = 100$ or more), while for a few loci ($L = 10$ or less) we already have enough coverage to make sampling error negligible.

is large (100 or 500), since when coverage is high read errors are compensated for (see Eq. (9).) In all cases we have studied the results are quite robust to DP errors, thus noise introduced by realistic pooling protocols should be easily overcome by the **CS** reconstruction.

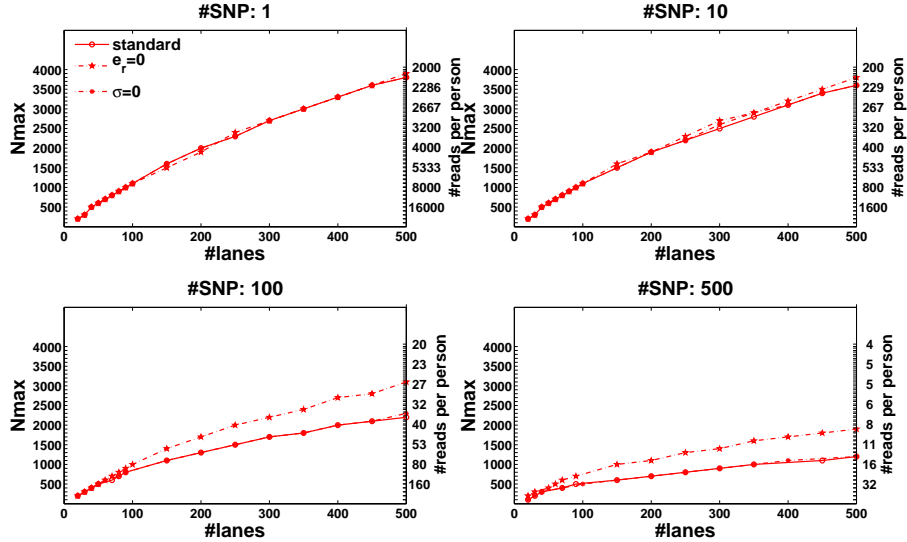


Figure 9: Effect of read errors and DP errors. The two dashed lines represent results obtained when assuming that reads are perfect and DP errors is zero, respectively. The solid line represents a realistic scenario with a read error of 1% and DP errors of $\sigma = 0.05$. While read error appears to have a significant factor in reducing N_{max} , the effect of DP errors seems to be negligible.

3.3 Modifying the sensing matrix

In all simulations presented so far we have considered the case where each pool includes approximately $N/2$ individuals. It may be desirable to minimize the number of individuals per pool [20], as this can lead to a faster and cheaper preparation of each pool. Here we shortly present the possibility of modifying M into a *sparse* sensing matrix, thus accommodating the requirement of having few individuals per pool.

Figure 10 presents the results of using only \sqrt{N} individuals in each pool, for the case $f = 1\%$ (marked as “ $\sqrt{N}, f = 1\%$ ”). For a small number of loci taken together ($L = 1$ or 10) the former dense Bernoulli(0.5) sensing matrix achieves higher N_{max} values. However, when the number of loci is large ($L = 100$ or 500) and for large number of lanes, it is preferable to use sparse pools of size \sqrt{N} . The same qualitative behavior was observed for $f = 0.1\%$ and $f = 2\%$. The success of sparse matrices in recovering the true genotypes is not surprising given theoretical and experimental evidence [3]. Further research is needed in order to determine the optimal sparsity of the sensing matrix for a given set of parameters.

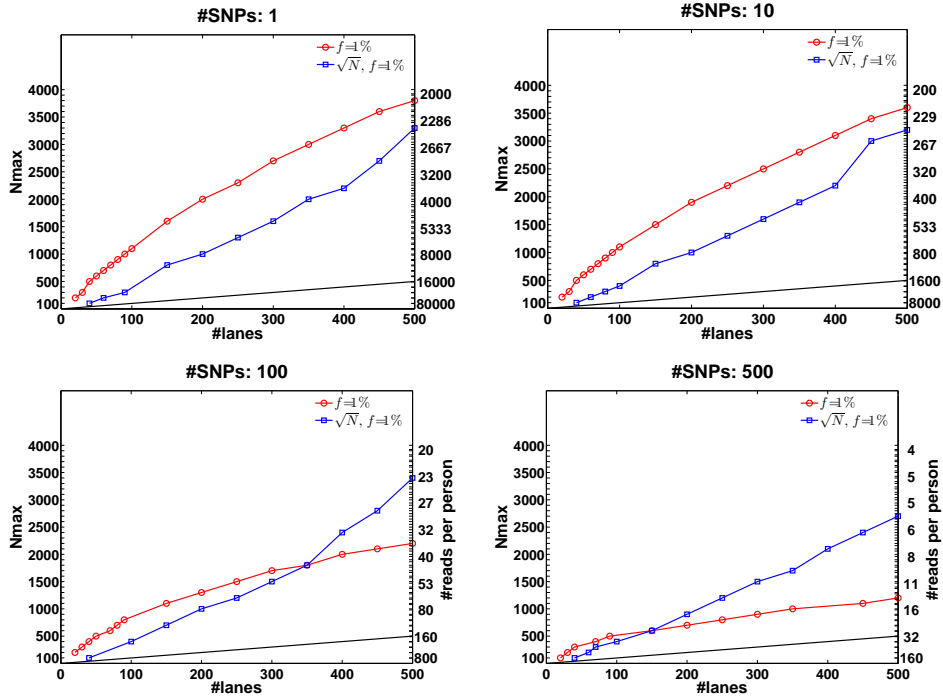


Figure 10: The effect of applying pools of \sqrt{N} or $N/2$ individuals (on average) for the case of $f = 1\%$. Overall, results are comparable, yet each pooling design is preferable for different settings of lanes and loci. The sparse (\sqrt{N}) design is more beneficial for large number of lanes and longer target regions. The average coverage on the right axis of each panel corresponds to the $N/2$ case. The coverage in the \sqrt{N} case is much larger since the total number of reads R is divided among a smaller number of individuals.

3.4 Combining barcodes and CS

Barcodes may also be combined with **CS** so as to improve efficiency and further reduce the number of required lanes. The DNA in each pool (as opposed to the DNA of a specific individual) may be tagged using a unique barcode (see Section 2.6.) Hence, in case we have n_{bar} different barcodes available, we apply n_{bar} pools to a single lane, with the price being that each pool contains only R/n_{bar} reads. Figure 11 displays N_{max} as a function of the number of lanes, for different values of n_{bar} , and for different rare allele frequencies.

The black line in each figure represents the “naive” capacity, which is simply $k \times n_{bar}$. Incorporating even a small number of barcodes into our **CS** framework results in a dramatic increase in N_{max} . For the same problem parameters but without using barcodes, could not recover the minimal possible number of individuals $N_{max} = 1000$ for $f = 0.1\%$ and could not reach more than $N_{max} = 100$ for $f = 1\%, 2\%$ (see Figs. 3,6.) Similarly to the non-barcodes case, the advantage over the naive approach is most prominent for $f = 0.1\%$, but is still significant for $f = 1\%, 2\%$. As the number of barcodes increases, the difference in performance between different sparsities f becomes smaller. As long as the coverage is kept high, it is still beneficial to increase the number of barcodes, as it effectively increases linearly the number of lanes. At a certain point, when many different barcodes are present in a single lane, coverage drops and sampling error becomes significant, hence the advantage of adding more barcodes starts to diminish.

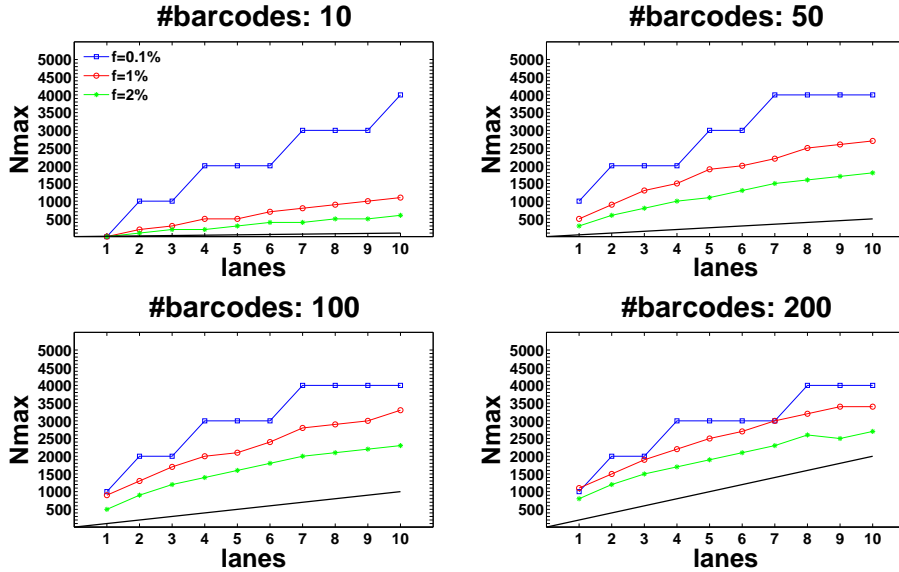


Figure 11: Results obtained by combining the **CS** approach with barcoding for $L = 1$. Barcoding improves results by enabling a higher number of ‘effective’ lanes (although these lanes contain a smaller number of reads.) The effect of adding a large number of barcodes is more pronounced for high minor-allele frequency. For example, at $f = 2\%$ and with 7 lanes, we can treat roughly 300 individuals with 10 barcodes, but around 2500 individuals with 200 barcodes. The increase in power is sub-linear, as is seen by the fact that when we add more barcodes, the performance becomes closer to that of the naive approach (shown in black) which increases linearly with the number of lanes. Still, only at a very high number of barcodes the naive approach can perform as well as the **CS** design.

4 Discussion

We have presented a method for identifying rare allele carriers via **CS**-based group testing. The method naturally deals with all possible scenarios of multiple carriers and heterozygous or homozygous rare alleles. Our results display the advantages of the approach over the naive one-individual-per-lane scenario: it is particularly useful for the case of a large number of individuals and low frequencies of rare alleles. We have also shown that our method can benefit from the addition of barcodes for different pools [20], and still improve upon ‘standard’ barcoding.

We view our main contribution as outlining a generic approach that puts together sequencing and **CS** for solving the problem of carrier identification. Following this mapping we may apply the vast amount of **CS** literature and benefit from any advancement in this rapidly growing field. We believe this is a major advantage over more ‘tailored’ approaches, e.g. [20, 44], although these methods may be superior to ours in specific cases.

Our method is *simple* in the sense that it applies **CS** in the most straightforward fashion. We have used an off-the-shelf **CS** solver and did not try to optimize any **CS** related parameter for the different scenarios - all parameters were kept fixed for all types of simulations thus optimizing reconstruction algorithms is likely to improve our results. Moreover, the method’s performance as detailed in Section 3 may be further improved, since our formulation of the **CS** problem has incorporated only part of the available information at hand. Using additional information may reduce the number of lanes or total reads needed to achieve a certain accuracy, as well as enable faster algorithms for reconstruction, thus allowing us to deal with larger sample sizes and larger regions.

As an example, the information that the input signal is trinary $(0, 1, 2)$ was considered only in the post-processing step after running GPSR, although it may be incorporated into the optimization procedure itself. Since most alleles are approximately distributed according to HW equilibrium, the frequency of 2’s, derived from the frequency of 1’s is very low, and the input vector is most often Boolean. Therefore, we could also modify the optimization so as to ‘punish’ for deviations from this pattern. In addition, we have treated each rare allele independently, although in case alleles originate from the same genomic region, one could use linkage disequilibrium information and reconstruct haplotypes. For example, if two individuals share a rare allele at position i , they are also likely to share an allele, probably rare, at position $i + 1$. It would be a challenge to add these constraints and enable the reconstruction of several adjacent loci simultaneously. Another improvement may stem from more accurate modeling of specific errors of sequencing machines, including quality scores which provide an estimate of error probability of each sequenced base [6, 31]. Such careful modeling typically results in far smaller error rates than the ones we have conservatively used ($\sim 0.5\% - 1\%$).

Another possible improvement may be to apply adaptive group testing, namely to decide whether to use lane k , based on reconstruction results of lanes $1, \dots, k - 1$. This enables an adaptation to unknown sparsity by simply generating pools one by one, each time solving the **CS** problem and checking if we get a sparse and robust solution. Once the solution stabilizes, we can stop our experiments thus not ‘wasting’ unnecessary lanes

(it may also be beneficial to change the pooling design of the next measurement and allow deviations from the randomized construction we have shown, once statistical information regarding the likely carriers is starting to accumulate).

The drawbacks of our method stem from the limitations of **CS** and sequencing technology. First of all, in case rare allele frequency is high enough, the sparsity assumption at the heart of the **CS** theory breaks down, and it may be problematic for **CS** to reconstruct the signal. The highest frequency possible for **CS** to perform well in this application was not determined, but one should expect a certain frequency above which it is no longer beneficial to apply **CS** and the naive one-individual-per-lane approach is preferable. The simulations we have performed estimate this frequency to be over 5% in most cases, thus taking effect only for the case of *common* alleles.

The number of individuals pooled together and the length of the targeted regions are limited by the total capacity of a given lane. We have shown that efficient reconstruction is possible when a significant number of individuals is pooled together, and when one can target efficiently a rather small genomic region. However, efficiency could be further improved if we could maintain a large enough coverage while further increasing the pool and region size. We expect that in the foreseeable future sequencing technology would yield higher number of reads per lane, which would allow larger pool size and genomic regions to be treated by our approach.

Another difficulty in our approach is related to the issue of randomness of the *sensing matrix* M . This randomness may be discarded by simply fixing a certain instance of the sensing matrix, although randomness in this case may be viewed as an advantage of **CS** - almost any (random) matrix would enable reconstruction, as opposed to intricate pooling schemes which need to be carefully designed.

The last drawback we should mention is related to the fact that each pool contains approximately half the individuals in the group. This may be problematic in cases where pooling preparation might be slow and costly, and we need to minimize the number of individuals in each pool [20]. In this case it may be interesting to apply a sparser pooling design. As shown in Section 3.3 there are scenarios in which it is advantageous to assign only \sqrt{N} individuals to a pool. Therefore, one needs to optimize the pool design together with other parameters, e.g. number of loci and lanes considered. This issue remains for future study.

Another major direction we intend to pursue is to test the **CS** approach experimentally. To the best of our knowledge, no available data is completely suitable for our purposes, thus we can not ‘adapt’ current data sets and ‘simulate’ such an experiment. Our approach is most beneficial for relatively high coverage and a large number of individuals, thus designing a suitable experiment is needed.

Finally, while we have demonstrated the benefits of **CS**-based group testing approach for genotyping, any genetic or epigenetic variant is amenable to our approach, as long as it can be detected by next generation sequencing technology and is rare in the population of interest. For example, Copy Number Variations (CNVs), important for studying both normal population variations and alterations occurring in cancerous tissues, provide a natural extension to our framework. In this case the number of reads serves as a proxy

to the copy number at a given locus, and the vector to be reconstructed contains the (integer) copy number levels of each individual, rather than their genotypes. Another example is given by rare translocations, often present in various tumor types - where an evidence for a translocation may be provided by a read whose head is mapped to one genomic region and whose tail is mapped to another distal region (or by two paired-end reads, each originating from a different genomic region.) Carriers of a particular rare translocation may be discovered using this approach. The extension of our method to these and perhaps other novel applications provides an exciting research direction we plan to pursue in the future.

References

- [1] T.J. Albert, M.N. Molla, D.M. Muzny, L. Nazareth, D. Wheeler, X. Song, T.A. Richmond, C.M. Middle, M.J. Rodesch, C.J. Packard, G.M. Weinstock, and Gibbs R.A. Direct selection of human genomic loci by microarray hybridization. *Nature Methods*, 4(11):903–905, 2007.
- [2] S. Becker, J. Bobin, and E.J. Candes. NESTA: A Fast and Accurate First-order Method for Sparse Recovery. *Arxiv preprint arXiv:0904.3367*, 2009.
- [3] R. Berinde and P. Indyk. Sparse recovery using sparse random matrices. *preprint*, 2008.
- [4] J. Bobin, J.L. Starck, and R. Ottensamer. Compressed sensing in astronomy. *Journal of Selected Topics in Signal Processing*, 2:718–726, 2008.
- [5] W. Bodmer and C. Bonilla. Common and rare variants in multifactorial susceptibility to common diseases. *Nature genetics*, 40(6):695–701, 2008.
- [6] W. Brockman, P. Alvarez, S. Young, M. Garber, G. Giannoukos, W.L. Lee, C. Russ, E.S. Lander, C. Nusbaum, and D.B. Jaffe. Quality scores and SNP detection in sequencing-by-synthesis systems. *Genome Research*, 18(5):763, 2008.
- [7] P.R. Burton, D.G. Clayton, L.R. Cardon, N. Craddock, P. Deloukas, A. Duncanson, D.P. Kwiatkowski, M.I. McCarthy, W.H. Ouwehand, N.J. Samani, et al. Genome-wide association study of 14,000 cases of seven common diseases and 3,000 shared controls. *Nature*, 447(7145):661–678, 2007.
- [8] E.J. Candes. Compressive sampling. In *Int. Congress of Mathematics*, pages 1433–1452, Madrid, Spain, 2006.
- [9] E.J. Candes, J. Romberg, and T. Tao. Stable signal recovery from incomplete and inaccurate measurements. *Arxiv preprint math/0503066*, 2005.
- [10] E.J. Candes, M. Rudelson, T. Tao, and R. Vershynin. Error correction via linear programming. In *Annual Symposium on Foundations of Computer Science*, volume 46, pages 295–308. IEEE Computer Society Press, 2005.

- [11] E.J. Candes and T. Tao. Decoding by linear programming. *IEEE Transactions on Information Theory*, 51(12):4203–4215, 2005.
- [12] E.J. Candes and T. Tao. Near-optimal signal recovery from random projections: Universal encoding strategies? *IEEE Transactions on Information Theory*, 52(12):5406–5425, 2006.
- [13] J.C. Cohen, R.S. Kiss, A. Pertsemlidis, Y.L. Marcel, R. McPherson, and H.H. Hobbs. Multiple rare alleles contribute to low plasma levels of HDL cholesterol. *Science*, 305(5685):869–872, 2004.
- [14] W. Dai, M.A. Sheikh, O. Milenkovic, and R.G. Baraniuk. Compressive sensing dna microarrays. *EURASIP Journal on Bioinformatics and Systems Biology*, 2009:oi:10.1155/2009/162824, 2009.
- [15] D.L. Donoho. Compressed sensing. *IEEE Transaction on Information Theory*, 52(4):1289–1306, 2006.
- [16] D.L. Donoho. For most large underdetermined systems of linear equations the minimal l_1 -norm solution is also the sparsest solution. *Communications on Pure and Applied Mathematics*, 59(6):797–829, 2006.
- [17] D.L. Donoho and J. Tanner. Sparse nonnegative solution of underdetermined linear equations by linear programming. *Proceedings of the National Academy of Sciences*, 102(27):9446–9451, 2005.
- [18] D. Du and F.K. Hwang. *Combinatorial group testing and its applications*. World Scientific Pub., 2000.
- [19] M. Duarte, M. Davenport, D. Takhar, J. Laska, T. Sun, K. Kelly, and R. Baraniuk. Single-pixel imaging via compressive sampling. *IEEE Signal Processing Magazine*, 25(2):83–91, 2008.
- [20] Y. Erlich, K. Chang, A. Gordon, R. Ronen, O. Navon, M. Rooks, and G.J. Hannon. Dna Sudoku-harnessing high-throughput sequencing for multiplexed specimen analysis. *Genome Research*, doi:10.1101/gr.092957.109, 2009.
- [21] M.A.T. Figueiredo, R.D. Nowak, and S.J. Wright. Gradient projection for sparse reconstruction: Application to compressed sensing and other inverse problems. *IEEE Journal of Selected Topics in Signal Processing*, 1(4):586–597, 2007.
- [22] W.M. Freeman, S.J. Walker, and K.E. Vrana. Quantitative RT-PCR: pitfalls and potential. *Biotechniques*, 26:112–125, 1999.
- [23] A.C. Gilbert, M.A. Iwen, and M.J. Strauss. Group testing and sparse signal recovery. In *42nd Asilomar Conference on Signals, Systems, and Computers*, Monterey, CA, 2008.

- [24] A.C. Gilbert and M.J. Strauss. Group testing in statistical signal recovery. *Technometrics*, 2006. submitted.
- [25] A. Gnirke, A. Melnikov, J. Maguire, P. Rogov, E.M. LeProust, W. Brockman, T. Fennell, G. Giannoukos, S. Fisher, C. Russ, S. Gabriel, D.B. Jaffe, E.S. Lander, and C. Nusbaum. Solution hybrid selection with ultra-long oligonucleotides for massively parallel targeted sequencing. *Nature Biotechnology*, 27(2):182–189, 2009.
- [26] K.L. Gunderson, S. Kruglyak, M.S. Graige, F. Garcia, B.G. Kermani, C. Zhao, D. Che, T. Dickinson, E. Wickham, J. Bierle, et al. Decoding randomly ordered DNA arrays. *Genome Research*, 14(5):870–877, 2004.
- [27] M. Hamady, J.J. Walker, J.K. Harris, N.J. Gold, and R. Knight. Error-correcting barcoded primers for pyrosequencing hundreds of samples in multiplex. *Nature Methods*, 5(3):235–237, 2008.
- [28] T.D. Harris, P.R. Buzby, H. Babcock, E. Beer, J. Bowers, I. Braslavsky, M. Causey, J. Colonell, J. DiMeo, J.W. Efcavitch, et al. Single-molecule DNA sequencing of a viral genome. *Science*, 320(5872):106–109, 2008.
- [29] J.N. Hirschhorn and M.J. Daly. Genome-wide association studies for common diseases and complex traits. *Nature Reviews Genetics*, 6(2):95–108, 2005.
- [30] M. Ingman and U. Gyllenstein. SNP frequency estimation using massively parallel sequencing of pooled dna. *European Journal of Human Genetics*, 17(3):383–386, 2009.
- [31] W.C. Kao, K. Stevens, and Y.S. Song. Bayescall: A model-based basecalling algorithm for high-throughput short-read sequencing. *Genome Research*, doi:10.1101/gr.095299.109, 2009.
- [32] S.J. Kim, K. Koh, M. Lustig, S. Boyd, and D. Gorinevsky. An interior-point method for large-scale l1-regularized least squares. *IEEE Journal of Selected Topics in Signal Processing*, 1(4):606–617, 2007.
- [33] R.J. Klein, C. Zeiss, E.Y. Chew, J.Y. Tsai, R.S. Sackler, C. Haynes, A.K. Henning, J.P. SanGiovanni, S.M. Mane, and Mayne, S.T. et al. Complement factor H polymorphism in age-related macular degeneration. *Science*, 308(5720):385–389, 2005.
- [34] B. Li and S.M. Leal. Discovery of Rare Variants via Sequencing: Implications for the Design of Complex Trait Association Studies. *PLoS Genetics*, 5(5):e1000481, 2009.
- [35] H. Li, J. Ruan, and R. Durbin. Mapping short DNA sequencing reads and calling variants using mapping quality scores. *Genome Research*, 18(11):1851–1858, 2008.
- [36] T.T. Lin and F.J. Herrmann. Compressed wavefield extrapolation. *Geophysics*, 72, 2007.

- [37] M. Lustig, D.L. Donoho, and J.M. Pauly. Sparse mri: The application of compressed sensing for rapid MR imaging. *Magnetic Resonance in Medicine*, 58:1182–1195, 2007.
- [38] E.R. Mardis. The impact of next-generation sequencing technology on genetics. *Trends in Genetics*, 24(3):133–141, 2008.
- [39] M. Margulies, M. Egholm, W.E. Altman, S. Attiya, J.S. Bader, L.A. Bembien, J. Berka, M.S. Braverman, Y.J. Chen, Z. Chen, et al. Genome sequencing in microfabricated high-density picolitre reactors. *Nature*, 437(7057):376–380, 2005.
- [40] J.M. McClellan, E. Susser, and M.C. King. Schizophrenia: a common disease caused by multiple rare alleles. *The British Journal of Psychiatry*, 190(3):194–199, 2007.
- [41] S. Muthukrishnan. *Data streams: Algorithms and applications*. Now Publishers Inc, 2005.
- [42] S.B. Ng, E.H. Turner, P.D. Robertson, S.D. Flygare, A.W. Bigham, C. Lee, T. Shaffer, M. Wong, A. Bhattacharjee, E.E. Eichler, M. Bamshad, D.A. Nickerson, and J. Shendure. Targeted capture and massively parallel sequencing of 12 human exomes. *Nature*, doi:10.1038/nature08250, 2009.
- [43] N. Norton, N.M. Williams, H.J. Williams, G. Spurlock, G. Kirov, D.W. Morris, B. Hoogendoorn, M.J. Owen, and M.C. O’Donovan. Universal, robust, highly quantitative SNP allele frequency measurement in DNA pools. *Human genetics*, 110(5):471–478, 2002.
- [44] S. Prabhu and I. Pe’er. Overlapping pools for high-throughput targeted resequencing. *Genome Research*, doi:10.1101/gr.088559.108, 2009.
- [45] S.H. Shaw, M.M. Carrasquillo, C. Kashuk, E.G. Puffenberger, and A. Chakravarti. Allele frequency distributions in pooled DNA samples: applications to mapping complex disease genes. *Genome Research*, 8(2):111–123, 1998.
- [46] R. Sladek, G. Rocheleau, J. Rung, C. Dina, L. Shen, D. Serre, P. Boutin, D. Vincent, A. Belisle, and Hadjadj, S. et al. A genome-wide association study identifies novel risk loci for type 2 diabetes. *Nature*, 445(7130):881–885, 2007.
- [47] H. Yang and C.S.J. Fann. Association mapping using pooled DNA. *Methods in Molecular Biology*, 376:161–175, 2007.

A Coping with unknown read error

We assume that the read error e_r is unknown to the researcher, but is constant across all lanes. One can introduce a slight modification to our procedure, which enables the learning of e_r from our pooling data. We replace \mathbf{z} in Eq. (7) by the convolution:

$$\mathbf{z} * e_r \equiv \mathbf{z} + e_r - 2\mathbf{z}e_r \quad (13)$$

The additive factor $e_r - 2\mathbf{z}e_r$ is different for different values of \mathbf{z} , but its dominant part is e_r . We can approximate it by $x_{N+1} \equiv e_r - 2\bar{z}e_r$, obtained from averaging the term $2\mathbf{z}e_r$ over all \mathbf{z} values (i.e. \bar{z} is the mean value of the vector \mathbf{z}). We can now reformulate the **CS** problem by adding one extra variable. Specifically, the unknown vector \mathbf{x} is replaced by $\mathbf{x}' = (\mathbf{x}, x_{N+1})$ and Eq. (7) is replaced by:

$$\mathbf{x}'^* = \underset{\mathbf{x}'}{\operatorname{argmin}} \|\mathbf{x}'\|_1 \quad s.t. \quad \left\| \frac{1}{2}\hat{M}'\mathbf{x}' - \frac{1}{r}\mathbf{z}' \right\|_2 \leq \epsilon \quad (14)$$

where M' is built from M by adding a constant column to its right as its $N + 1$'s column with all its values set to -1 .